PHILOSOPHICAL TRANSACTIONS OF THE ROYAL SOCIETY A

Phil. Trans. R. Soc. A (2011) **369**, 1925–1942
doi:10.1098/rsta.2011.0006

Quantifying greenhouse-gas emissions from atmospheric measurements: a critical reality check for climate legislation

By Ray F. Weiss[1,*] and Ronald G. Prinn[2]

[1]*Scripps Institution of Oceanography, University of California, San Diego, La Jolla, CA 92093-0244, USA*
[2]*Center for Global Change Science, Massachusetts Institute of Technology, Building 54-1312, Cambridge, MA 02139-4307, USA*

Emissions reduction legislation relies upon 'bottom-up' accounting of industrial and biogenic greenhouse-gas (GHG) emissions at their sources. Yet, even for relatively well-constrained industrial GHGs, global emissions based on 'top-down' methods that use atmospheric measurements often agree poorly with the reported bottom-up emissions. For emissions reduction legislation to be effective, it is essential that these discrepancies be resolved. Because emissions are regulated nationally or regionally, not globally, top-down estimates must also be determined at these scales. High-frequency atmospheric GHG measurements at well-chosen station locations record 'pollution events' above the background values that result from regional emissions. By combining such measurements with inverse methods and atmospheric transport and chemistry models, it is possible to map and quantify regional emissions. Even with the sparse current network of measurement stations and current inverse-modelling techniques, it is possible to rival the accuracies of regional 'bottom-up' emission estimates for some GHGs. But meeting the verification goals of emissions reduction legislation will require major increases in the density and types of atmospheric observations, as well as expanded inverse-modelling capabilities. The cost of this effort would be minor when compared with current investments in carbon-equivalent trading, and would reduce the volatility of that market and increase investment in emissions reduction.

Keywords: global warming; greenhouse-gas emissions; climate legislation

1. Introduction

Entering the second decade of the twenty-first century, legislation to stem the adverse effects of anthropogenic climate change by requiring reductions in anthropogenic carbon dioxide (CO_2) and non-CO_2 long-lived greenhouse-gas (GHG) emissions is becoming increasingly widespread. In addition to the multi-national Kyoto Protocol, established under the United Nations Framework

*Author for correspondence (rfweiss@ucsd.edu).

One contribution of 17 to a Discussion Meeting Issue 'Greenhouse gases in the Earth system: setting the agenda to 2030'.

Convention on Climate Change (UNFCCC), there are many national, bilateral, multi-lateral and regional initiatives to limit GHG emissions. Emissions of non-CO_2 GHGs, many of which have global warming potentials (GWPs) that are tens to thousands of times greater than CO_2 per unit mass, represent roughly 35 per cent of current GHG emissions on a carbon-equivalent basis [1], and play a significant role in the current emissions trading market. Among the long-lived non-CO_2 GHGs are a number of high-GWP anthropogenic gases that are not regulated by the Kyoto Protocol, but which still contribute significantly to anthropogenic radiative forcing, especially the chlorofluorocarbons (CFCs) and other stratospheric ozone-depleting substances that are regulated by the Montreal Protocol.

Current emissions reduction legislation is based on accounting methods that are prescribed under the UNFCCC for calculating inventories of emissions of industrial and biogenic GHGs at their sources, so-called 'bottom-up' emissions reporting. Detailed guidelines for emissions reporting have been developed under the auspices of the Intergovernmental Panel on Climate Change (IPCC; [2] and subsidiary volumes). These prescribed procedures are based on activity metrics such as economic and land-use databases, emission factors relating these activities to GHG emissions, and time delays between GHG production and release. There is capacity for including uncertainties in these estimates, but they are often reported as 'unknown'. This is a complex task involving estimates for a very wide range of GHG emission sources; each reported individually and then aggregated. The resulting national GHG emission inventories for UNFCCC Annex I developed countries are reported with many digits of resolution, but usually without uncertainties [3]. However, estimated emissions of GHGs of primarily industrial origin and with limited types of sources are generally held to have greater accuracy than emissions of GHGs from primarily biogenic sources that are more difficult to quantify.

It is important to note that the Kyoto Protocol and other similar legislation requires carbon-equivalent emissions reductions relative to a base period that are often specified with resolutions of 5 per cent or less, with required 'certification' according to the IPCC or other formal bottom-up reporting procedures. But do these procedures yield actual emissions? This is a critical question because the anthropogenic affect on climate is ultimately driven by actual emissions of GHGs to the atmosphere, not by reported ones.

2. Emission estimation approach

For emissions control legislation to be effective, and considering that enforcement is likely to be practical only by bottom-up methods, it is essential that significant discrepancies between bottom-up emissions estimates and 'top-down' emissions estimates based on atmospheric measurements be resolved. But because emissions control legislation is national or regional in nature, not global, it is also essential that top-down emission estimates be determined at these same geographic scales. Atmospheric GHG measurements and inverse modelling, when proceeding in tandem, allow observations to be used to answer important scientific, as well as regional, emission questions. Modelling can also help to define measurement strategies (target species, site location, measurement precision and frequency)

and priorities. Using the so-called minimum variance Bayesian inverse methods, optimal estimates of fluxes by process and/or region in a chemical transport model (CTM) can be obtained by minimizing the errors (variances) in the estimated emissions given the errors in the observations. These inverse studies can use measurements from a number of independent observational networks, after conversion to a common calibration scale using results of inter-laboratory measurement comparisons.

(*a*) *Statistical methods*

There are a number of statistical approaches to flux (source and sink) estimations [4–6]. As an illustration here, we discuss specifically the discrete Kalman filter (DKF). A desirable feature of the DKF is its capability for objective estimation of the errors in the estimated fluxes and for inclusion of both observational and certain CTM errors in the measurement error treatment. A detailed introduction to the DKF in vector/matrix form for application to estimating sources and sinks for atmospheric trace gases can be found in Prinn [6]. To illustrate some of the key aspects of the use of the DKF for emissions estimation, we can look at the highly simplified but informative one-dimensional case of estimating sequential emissions from a single region using a sequence of observations at a single site where vectors and matrices are now replaced by scalars.

In this case, the filter is effectively minimizing the square of the error ($p_k = \sigma_{xk}^2$) in the estimated emissions (x_k) at discrete time k. We define y_k^{o} as the 'observation' (mole fraction) at time k, r_k as the square of the error in the observation at time $k (r_k = (\sigma_{yk}^{\mathrm{o}})^2)$, x_k^{f} as the 'forecast' value for x_k (value before using observation k), x_k^{a} as the 'analysis' value for x_k (corrected value after using observation k), $h_k = \mathrm{d}y_k/\mathrm{d}x_k$ (sensitivity of model mole fraction to model emissions) and $y_k = h_k x_k^{\mathrm{f}}$ as the model estimate for observation k. If we also define p_k^{f} and p_k^{a} as the forecast and analysis values, respectively, for p_k (values before and after using observation k) and m as a scalar that multiplies the analysis values from a prior time step to serve as a forecast for the current time step, then the recursive filter equations to estimate emissions and their errors are simply

$$x_k^{\mathrm{f}} = m_{k-1} x_{k-1}^{\mathrm{a}}, \tag{2.1}$$

$$x_k^{\mathrm{a}} = x_k^{\mathrm{f}} + k_k (y_k^{\mathrm{o}} - h_k x_k^{\mathrm{f}}), \tag{2.2}$$

$$k_k = \frac{p_k^{\mathrm{f}} h_k}{h_k^2 p_k^{\mathrm{f}} + r_k} = \frac{1}{h_k + r_k/(h_k p_k^{\mathrm{f}})} = \text{Kalman gain (scalar) at time } k, \tag{2.3}$$

$$p_k^{\mathrm{f}} = m_{k-1}^2 p_{k-1}^{\mathrm{a}} \tag{2.4}$$

and

$$p_k^{\mathrm{a}} = (1 - k_k h_k) p_k^{\mathrm{f}} = \left(1 - \frac{1}{1 + [r_k/(h_k^2 p_k^{\mathrm{f}})]}\right) p_k^{\mathrm{f}}. \tag{2.5}$$

Note that because $p_k^{\mathrm{a}} \le p_k^{\mathrm{f}}$, then the square of the error in the estimated emissions after use of the observation is less than its forecast value. In addition, for the desired large p_k reduction (or large reductions in emission errors from their forecasts), we want $r_k \ll h_k^2 p_k^{\mathrm{f}}$. For the desired large emission correction

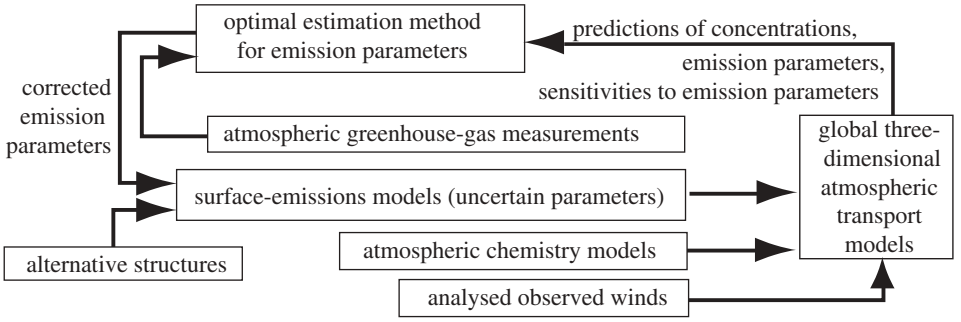

Figure 1. Schematic illustrating the general inverse method for estimating emission fluxes or parameters. The Kalman filter is an example of an optimal estimation method. The concentrations, emission parameters and sensitivities to emission parameters refer to y, x and $\mathrm{d}y/\mathrm{d}x$ in the simple example discussed in the text. The Model of Atmospheric Transport and Chemistry (MATCH) model, containing an atmospheric chemistry sub-model where appropriate, and driven by analysed observed winds (National Centers for Environmental Prediction (NCEP), the European Centre for Medium Range Weather Forecasts (ECMWF)) is an example of a suitable three-dimensional model. Surface-emission models range from substantial codes that simulate the surface source and sink processes down to simple specifications of time- and space-varying emissions based on *in situ* flux measurements and information about anthropogenic sources. Alternative structures refer to different choices for the emission models.

$(x_k^{\mathrm{a}} - x_k^{\mathrm{f}})$, for a given large difference $(y_k^{\mathrm{o}} - h_k x_k^{\mathrm{f}})$ between observation and model, we want the Kalman gain $k_k \to 1/h_k$ (its maximum value), which occurs when $r_k \ll h_k^2 p_k^{\mathrm{f}}$. That is, for both desirable outcomes, we want $(\sigma_{yk}^{\mathrm{o}})^2 \ll (\mathrm{d}y_k/\mathrm{d}x_k)^2(\sigma_{xk}^{\mathrm{f}})^2$ or equivalently $\sigma_{yk}^{\mathrm{o}} < (\mathrm{d}y_k/\mathrm{d}x_k)\sigma_{xk}^{\mathrm{f}}$ (i.e. the error in the observation y_k^{o} needs to be less than the error in the model value $y_k = h_k x_k^{\mathrm{f}}$ for the observation). A schematic of the general approach is given in figure 1.

It is important to ensure that model and observation imperfections are accounted for properly (e.g. [4,6]). The processes and parameters to be estimated are chosen so that they have effects on the emission patterns in space and time that are sufficiently distinct from each other to ensure uniqueness and stability (e.g. [7,8]). The estimations are also formulated so that small fractional changes in concentrations do not yield unacceptably large fractional changes in deduced emissions. Observational uncertainties that are associated with absolute calibration, instrument precision and inadequate sampling in space and time are incorporated into the observation error whenever possible. It is also important to recognize when observation errors are correlated, thus possibly violating a condition of optimal filters like the DKF or complicating the definition of the observational error treatment. Various methods exist to address this (see [4,6] for reviews). Weak nonlinearities in the chemical models (e.g. the lowering of the hydroxyl radical (OH) when methane (CH_4) emissions increase) are routinely handled by recalculating the time-dependent sensitivities (h_k in the above simplified equations) after each run through all the data, and repeating the inverse method to ensure convergence. Structural errors and random and systematic transport errors (i.e. errors in h_k above) are handled through utilization of multiple model versions and Monte Carlo methods (e.g. [9]) and/or by increasing the measurement error to include the error owing to the model (e.g. [6,10]).

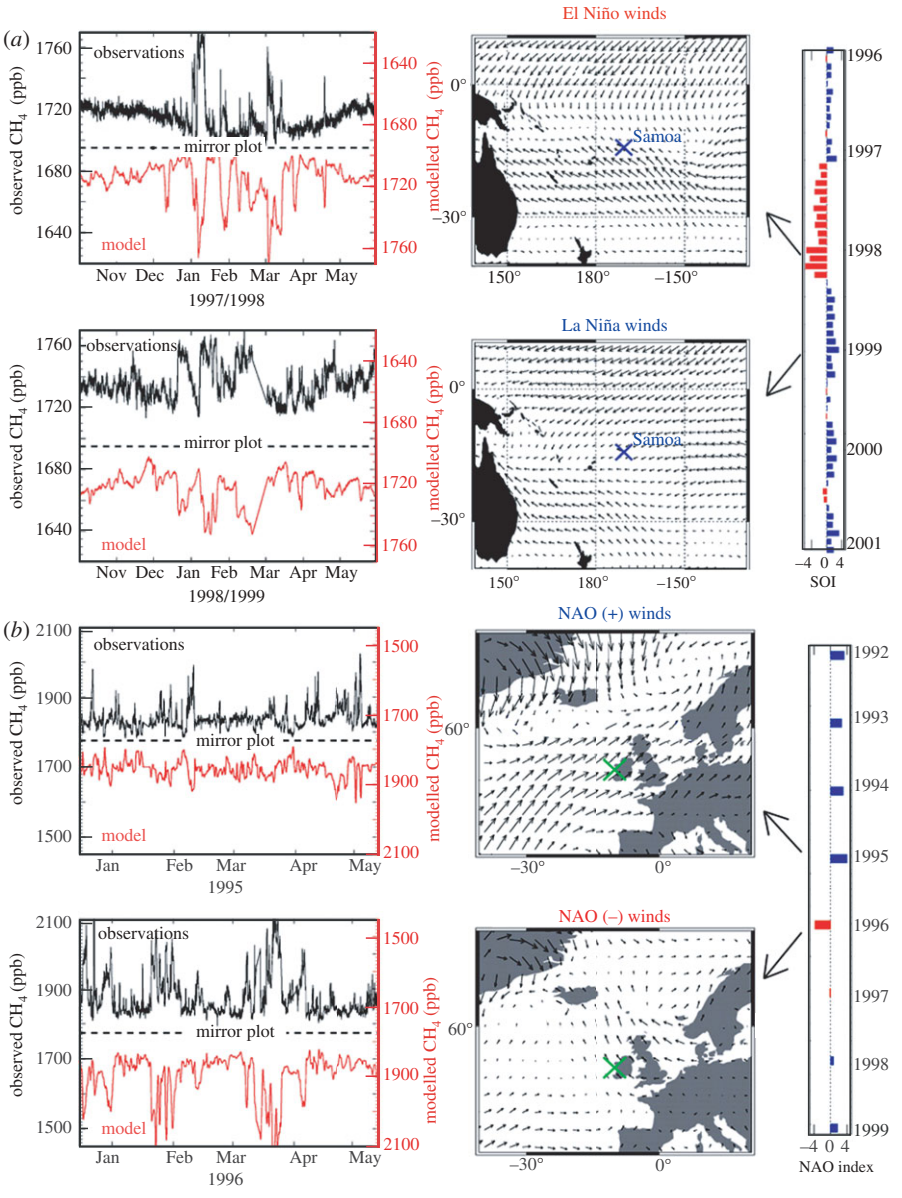

Figure 2. MATCH simulates the very significant effects of temporal and inter-annual variability of circulation patterns on atmospheric methane (CH_4) mole fractions. Advanced Global Atmospheric Gases Experiment (AGAGE) CH_4 observations (black) versus MATCH simulations (red) are shown at (*a*) Samoa and (*b*) Mace Head, Ireland [7,8]. The El Niño Southern Oscillation Index (SOI) and the North Atlantic Oscillation (NAO) index are shown adjacent, respectively. The comparison in (*a*) is for the same months during the 1998 El Niño (top) and 1999 La Niña (bottom) with the January–May average surface wind fields for the 2 years, and the comparison in (*b*) is for the same months during the 1995 positive NAO (top) and 1996 negative NAO (bottom) with the January–May average surface winds also shown. Note that observations and model estimates are plotted on scales of opposite direction so that an exact mirror image of the two datasets implies perfect agreement. The CH_4 measurement station location is shown by a cross on each surface wind field map.

(*b*) *Models*

A basic requirement for inverse modelling is an accurate and realistic multi-dimensional atmospheric CTM. Even apparently small transport errors can lead to significant errors in estimated sources or sinks [11,12]. Three-dimensional models are essential to resolve pollution events and solve for regional sources and sinks. In addition, three-dimensional models must possess realistic atmospheric circulations. These models may compute quantities at fixed grid points (Eulerian) or compute them following the trajectories of the air parcels (Lagrangian).

As an example of a three-dimensional Eulerian model, a large number of inverse studies have used the Model of Atmospheric Transport and Chemistry (MATCH) [10,13,14]. This is an offline global three-dimensional transport model that uses meteorological fields derived from forecast-centre analyses. MATCH has been successfully driven by meteorological data from the National Centers for Environmental Prediction (NCEP), the European Centre for Medium Range Weather Forecasts (ECMWF) and the Goddard Space Flight Center/National Aeronautics and Space Administration (GSFC/NASA) Data Assimilation Office (DAO) analysis [14]. Sub-grid mixing processes, which include dry convective mixing, moist convective mixing and large-scale precipitation processes, are computed in the model. MATCH can be used at a horizontal resolution as fine as T62 ($1.8^\circ \times 1.8^\circ$), with either 42 or 28 levels in the vertical. MATCH inversions have been used for many GHGs, including chlorofluorocarbon-11 (CF_3Cl) [10], CO_2 [15–18], CH_4 [7,8], nitrous oxide (N_2O) [19] and carbon tetrachloride (CCl_4) [20]. The ability of MATCH to accurately simulate the effects of transport on long-lived trace gases is well illustrated by the methane simulations in figure 2.

Another common modelling approach is based on back-trajectories computed from meteorological data using a Lagrangian model (e.g. [12]). By dividing the trace gas observations into 'background air events' and 'pollution events' and computing air mass back-trajectories, and thus air mass transit times over predefined emission regions, the time/space average emissions from these predefined regions can be determined. The method obviously requires accurate definition of both back-trajectories and eddy diffusive fluxes. The Hybrid Single-Particle Lagrangian Integrated Trajectory (HYSPLIT) model [21,22] of the National Oceanic and Atmospheric Administration (NOAA) has been used for this purpose [23]. The UK Met Office Lagrangian particle model (Numerical Atmospheric dispersion Modelling Environment; NAME) has also been applied extensively to determine European source and sink strengths for a variety of species (e.g. [24–29]). Similarly, Australian regional emissions of various species have been determined using inverse studies and regional transport models [30,31]. The FLEXPART Lagrangian particle dispersion model has also been used to determine emissions of halocarbon GHGs regionally and globally (e.g. [32]).

While two-dimensional models are not suitable for regional emission estimation, they have their uses (e.g. solving for global or hemispheric emissions or for model error analysis). Three-dimensional models, being computationally expensive, do not always lend themselves well to doing very long time integrations, and multiple runs are required to address uncertainties (e.g. thousands of runs for Monte Carlo treatments of model transport, rate constant and absolute calibration errors). A two-dimensional model is better suited to a full uncertainty

analysis because its transport is 'tunable' to simulate observed latitudinal gradients (e.g. [9,33]). For example, measurements of N_2O have been used in conjunction with three-dimensional atmospheric CTMs transport models to attribute source and sink strengths [19,34], and use of a complementary two-dimensional model to assess the effects of model error using a Monte Carlo approach indicates that the errors emanating from the three-dimensional inversions alone need to be augmented significantly to account for model errors [19].

3. Global and regional emissions

There are large uncertainties associated with emissions of the biogenic components of some of the most important anthropogenic GHGs such as CO_2, CH_4 and N_2O—emissions associated with land-use changes, agriculture and waste processing. For these gases, there is also a need to separate anthropogenic emissions from natural emissions. As a result, the accuracies of bottom-up emissions inventories are most easily assessed for global emissions of purely industrial long-lived anthropogenic GHGs that are emitted from defined sources and are easily quantified from atmospheric measurements. Furthermore, emissions of industrial non-CO_2 GHGs, with their very high GWPs, are particularly important to quantify because they represent a disproportionately large share of the global carbon-equivalent trading market, even though their contributions to global warming are much less than that of CO_2.

Atmospheric abundances of a wide range of GHGs, including all of the non-CO_2 GHGs currently regulated by the Kyoto and Montreal Protocols, are routinely measured at a few select locations around the world by several independent research programmes including our Advanced Global Atmospheric Gases Experiment (AGAGE) programme [35,36]. These measurements, made in real time at remote stations, in flask samples and in archived air samples, yield accurate trends for the background atmospheric composition that extend back three decades for most of these gases. They can also be extended well before their industrial production when combined with measurements of air trapped in polar firn or ice cores (e.g. [37]). Using such data and the estimation approaches discussed above, it is possible to calculate top-down global emission rates from the measured trends, especially for long-lived gases with simple chemistry, and then to compare these values with the reported bottom-up emission rates.

The current knowledge of methane emissions exemplifies the issues surrounding gases with large biogenic, as well as anthropogenic, sources. After nearly a decade of little net change, the mole fractions of this gas began to rise in both hemispheres in 2006–2008 [38]. The inverse modelling by Rigby *et al.* [38] implied that the increase in growth rate was due either to increasing tropical and high-latitude emissions or to a smaller high-latitude emissions increase along with a few percent tropical OH decrease (or to some combination of the two). A later study of spatial gradients and Arctic isotopic signals by Dlugokencky *et al.* [39] suggested that the rise was primarily due to increased wetland emissions in both the high latitudes and tropics, with little influence from OH variations. Bousquet *et al.* [40]

earlier suggested that the stable period for CH_4 preceding 2006 was caused by a decreasing wetland source countering an increasing fossil-fuel-related source, with the sink of CH_4 owing to OH potentially playing a role in the observed atmospheric variability. For comparison, Chen & Prinn [8] attributed the CH_4 variations over 1996–2001 when compared with the literature values for the years before that to decreased fossil-fuel-related emissions and increased rice-paddy emissions, with the 1998 positive anomaly owing to increased global wetland and wildfire emissions. While the suggestion of very large methane emissions from vascular plants has been challenged [1], Chen & Prinn [8] have noted that their computed increased rice emissions (about 25 Tg methane yr^{-1}) could also be due to neighbouring non-rice wetland emissions.

The estimation of emissions for the essentially purely anthropogenic (industrial) greenhouse gases is more straightforward than for those gases whose budgets involve both biogenic and anthropogenic components. However, challenges still remain for accurately inferring regional emission estimates for these industrial gases. Examples for four high-GWP anthropogenic GHGs are presented here.

Carbon tetrafluoride (CF_4) is the longest-lived GHG regulated by the Kyoto Protocol, with an atmospheric lifetime of 50 000 years and a GWP of 7390 on a 100 yr time horizon [1]. It is emitted principally as a by-product of aluminium production, with lesser but significant emissions from the electronics industry. The trend of CF_4 concentration in the atmosphere is being measured in real time by AGAGE, and with the aid of stored samples, its trend in both hemispheres has been extended back to the 1970s [41]. There is also a small natural source of CF_4 from the continental lithosphere [42], which, because of its very long atmospheric lifetime, accounts for about half of the approximately 78 ppt (parts per trillion, dry air mole fraction) in the current atmosphere. But this flux is negligible when compared with the anthropogenic flux that drives the current trend. Modelling the AGAGE atmospheric CF_4 trends using a 12 box inverse model [41] yields a top-down global anthropogenic CF_4 emission flux that peaked in 1980 at about 18 Gg yr^{-1} and tapered to about 16 Gg yr^{-1} in 1990 and about 11 Gg yr^{-1} in 2006, with a modelled uncertainty of about 5 per cent. This modelled top-down global emission history is shown in figure 3, together with various reported bottom-up CF_4 emission estimates.

Comparison with bottom-up estimates reported to the UNFCCC by the Annex I industrialized countries [3] shows that in 1990, when reporting began, reported emissions accounted for only about 60 per cent of the measured atmospheric increase, and that by 2006, this fraction had decreased to about 40 per cent. In other words, while the rate of CF_4 accumulation in the atmosphere decreased by about 30 per cent during this period, the Annex I reported CF_4 emissions decreased by about 50 per cent. Although aluminium-producing countries like China, India and Brazil are not included in Annex I reporting, and production by these countries certainly increased significantly over this time period, it is difficult to reconcile that by 2006, non-Annex I countries accounted for about 60 per cent of global CF_4 emissions. Reinforcing this concern are the bottom-up results of the International Aluminium Institute (IAI) report series (e.g. [43]), which include worldwide CF_4 emissions from Annex I as well as non-Annex I aluminium production, but do not include emissions from the electronics industry. When the IAI estimates are added to the much smaller electronics

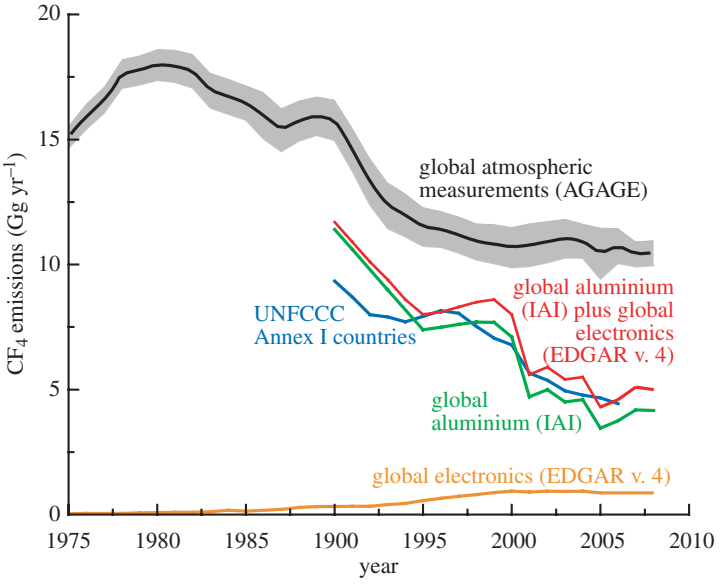

Figure 3. Top-down global emissions of carbon tetrafluoride (CF_4) modelled from global atmospheric measurements in the AGAGE programme [41], with shaded combined modelling and measurement uncertainties (±1 standard deviation), compared with the bottom-up global emissions estimates for the aluminium industry (e.g. [43]), for the electronics industry [44] and for these two sources combined. Also plotted are bottom-up emissions reported to the UNFCCC for the Annex I developed countries [3]. Adapted from Mühle *et al.* [41].

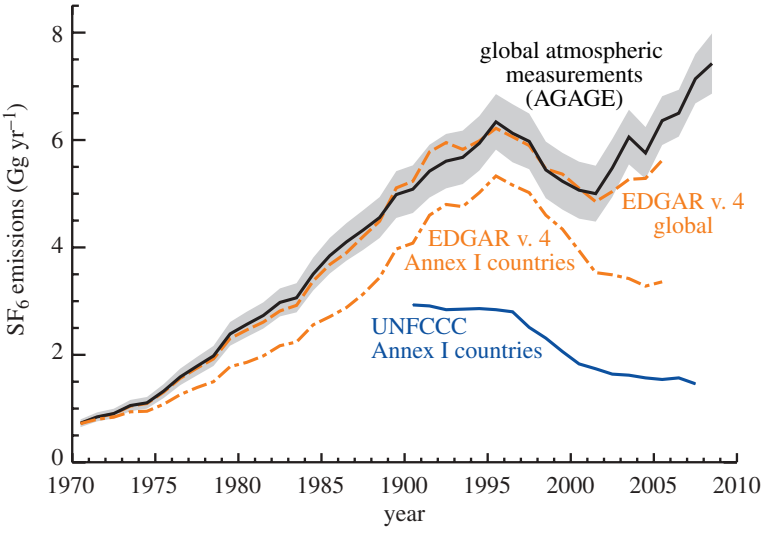

Figure 4. Top-down global emissions of sulphur hexafluoride (SF_6) modelled from AGAGE programme global atmospheric measurements [48], with shaded combined modelling and measurement uncertainties (±1 standard deviation) compared with bottom-up global emissions reported to the UNFCCC for the Annex I developed countries [3] after correction of pre-1995 reported Japanese emissions [46]. Also plotted are the EDGAR global-estimated emissions [44] that take into account bottom-up estimates as well as atmospheric measurements, and EDGAR estimates for SF_6 emissions only from Annex I countries that are roughly double those reported to the UNFCCC. Adapted from Rigby *et al.* [48].

industry global CF_4 emissions estimates compiled by v. 4.0 of the Emission Database for Global Atmospheric Research (EDGAR) [44], the results account for only about 75 per cent of the AGAGE measured increases in 1990, and by 2006, this fraction decreases to about 45 per cent. In other words, the combined IAI and EDGAR electronics estimates are in reasonable agreement with emissions reported to the UNFCCC, even though the former values include non-Annex I countries and the latter ones do not. For the most recent part of the record, neither of these sets of reported CF_4 emissions account for even half of the measured increase in the global atmosphere.

Sulphur hexafluoride (SF_6) is the most potent GHG regulated by the Kyoto Protocol, with a GWP on a 100 yr time horizon of 22 800 and an atmospheric lifetime of 3200 years [1]. It is used principally as a dielectric to prevent arcing in high-voltage equipment, and also in industrial applications where a heavy and chemically inert gas is required. SF_6 is also emitted naturally from the continental lithosphere, but in such small quantities relative to its atmospheric lifetime that its natural pre-industrial background concentration was less than 0.006 ppt [45]. Its present atmospheric abundance of about 6.8 ppt is therefore effectively entirely anthropogenic. Recent trends in global atmospheric SF_6 distributions have been measured and modelled extensively and independently by several research programmes, including the University of Heidelberg [46,47], AGAGE [48] and the NOAA Earth System Research Laboratory [49,50]. The SF_6 measurements of each of these three programmes are generally in good agreement and lead to essentially the same conclusion, namely that global SF_6 emissions are greatly underestimated by bottom-up emissions reported to the UNFCCC by Annex I countries.

The modelled SF_6 global emissions history based on AGAGE global atmospheric measurements [48] is compared with various bottom-up emissions estimates in figure 4. After correction of pre-1995 reported Japanese emissions [46], all the datasets show that throughout the mid-1990s, only about 40 per cent of total emissions were reported by Annex I countries, and that by 2006, this fraction had reduced to about 20–25%. If the Annex I countries have indeed reported correctly, then the non-Annex I countries emitted about 1.5 times as much SF_6 as the Annex I countries in the mid-1990s, and by 2006, they were emitting four or five times as much. A more likely explanation that is supported by the v. 4.0 EDGAR [44] interpretation of this mismatch is that Annex I SF_6 emissions are severely under-reported and that they actually represented about 80 per cent of the total in the mid-1990s and about 60 per cent of the total in 2006. In other words, the Annex I countries collectively have likely under-reported SF_6 emissions by more than a factor of 2.

With respect to the use of the EDGAR [44] database for comparisons of top-down and bottom-up emission fluxes, it is important to note that because EDGAR's objective is to provide the best emission estimates, both bottom-up and top-down methods are used to arrive at its recommended values of such parameters as emissions factors and emissions delays. Discrepancies such as the ones discussed above, in which measured global atmospheric trends have disagreed significantly with EDGAR bottom-up assessments, have resulted in major revisions of EDGAR emission values in subsequent release versions. For CF_4 and SF_6, the current (v. 4.0) EDGAR global total and Annex I emission estimates are neither bottom-up nor top-down, but rather are in effect a synthesis

of both, which improves upon the purely bottom-up approach by adjusting emission factors. In the case of SF_6, these relationships are discussed by Maiss & Brenninkmeijer [51] and Rigby *et al.* [48]

Nitrogen trifluoride (NF_3) is not regulated by the Kyoto Protocol, and its emissions from Annex I countries are therefore not required to be reported to the UNFCCC, but its long lifetime of about 550 years and high GWP of about 16 800 on a 100 yr time horizon [52], and its use as a replacement in electronics manufacturing for perfluorocarbons that are currently regulated, make it a strong candidate for future emissions regulation. The first measurements of the trend of NF_3 in the global atmosphere were made by the AGAGE programme [53]. They showed that its present global abundance is about 0.5 ppt and that its emissions in 2006 were roughly four times greater than the only published bottom-up global NF_3 emission estimate for that year. When recently unpublished industry-wide estimates of global NF_3 usage provided by Air Products Corporation, a major producer, are compared with the modelled global atmospheric NF_3 emission results, they suggest that about 9 per cent of current global NF_3 usage is emitted to the atmosphere, 4.5 times greater than the 2 per cent emission factor that has been used widely in bottom-up estimates [54].

Although each of the above examples finds significantly greater global emissions than are estimated by bottom-up accounting methods, this is not uniformly the case. Sulphuryl fluoride (SO_2F_2) is a fumigant that is used increasingly to kill termites and other pests, often as a replacement for methyl bromide, which is restricted by the Montreal Protocol because of its role in stratospheric ozone depletion. SO_2F_2 is not regulated by the Kyoto Protocol, and its emissions from Annex I countries are therefore not reported to the UNFCCC. The first measurements of SO_2F_2 in the global atmosphere [55], coupled with laboratory studies of its optical properties and reactivity [56], showed that its GWP is about 4800 on a 100 yr time horizon and its atmospheric lifetime is about 36 years. The observed global trend of SO_2F_2, presently at about 1.6 ppt and rising at about 5 per cent per year, is best explained by the emission to the atmosphere of only about two-thirds of its estimated global usage [55]. Either the usage data are overestimated, or unidentified mechanisms destroy about one-third of the gas before it is emitted to the atmosphere so that the flux to the atmosphere is reduced without changing the modelled atmospheric lifetime.

The picture that emerges from these four examples of global top-down and bottom-up comparisons for these industrial gases is that the discrepancies can be quite large, and that more often than not, the measured accumulations of industrially produced GHGs in the atmosphere are substantially greater than can be explained by the emissions that have been reported. Certainly, the discrepancies are large enough to call into serious question the reliability of the emission factors that are used in bottom-up emissions accounting, the many significant digits with which these emissions are typically reported, and the viability of GHG emissions reduction legislation that depends solely on bottom-up reporting procedures. Also called into question are the viability of emissions trading that depends upon bottom-up emissions accounting, and the feasibility of implementing legislation that requires reductions in emissions that are small when compared with the ability of prescribed bottom-up methods to resolve them.

4. Future prospects for improvements

The uncertainties of current regional emission estimates either by top-down or bottom-up approaches are commonly greater than 10–20%—sometimes very much greater—and thus are grossly inadequate for verifying claims of emission reductions by nations (e.g. mandated reductions under the Kyoto Protocol are generally only a few to 10%).

Looking to the future, it is clear that the spatial density of precise high-frequency atmospheric trace-gas measurements, whether using *in situ* or remotely sensed methods, needs to be increased by an order of magnitude or more. Equally important, the knowledge (theory, observation) embraced in models of industrial or ecosystem fluxes should be incorporated into the model system to enable estimation of uncertain parameters in these flux models as opposed to simply the fluxes themselves. In essence, this approach combines the best features of the bottom-up and top-down methods in flux estimation. Specifically, the use of an adjoint of MATCH or other similar model, coupled to models of the surface fluxes, would enable the estimation of uncertain parameters or controls in the flux model with a more powerful statistical approach. An adjoint of a model code is a complementary code that relates anomalies in model outputs (e.g. mole fractions) to changes in model inputs (e.g. emissions) or model parameters. Using the mathematical algorithms (but not the exact goal) of control theory (e.g. [57]), one can formulate the state estimation problem using a cost function J (p_k in the simplified discussion earlier) that is augmented with a demand for model consistency using the so-called Lagrange multipliers. Any variable that can be affected by changes in any of the control variables is called active, while variables that remain unaffected are called passive. Thus, the computations consist of an active part in which the coupling of the surface fluxes or atmospheric destruction rates is considered and that would be improved as part of the estimation problem to minimize J, and a passive part in which all the other elements of the system are considered that do not change throughout the optimization (e.g. the MATCH atmospheric circulation).

Through variation of the controls and initial conditions of the system, a solution of the state vector (x_k in the simplified discussion earlier) is sought that minimizes J. The general structure of J consists of four sums measuring: (i) the departure of the initial state from a first guess, (ii) the difference between the observations and the model projections of them, (iii) the deviation of the controls from a prior, and (iv) the demand that the state vector satisfies the various model equations through the introduction of Lagrange multipliers. Besides its key role in the J-minimization process, and thus in the state vector and model parameter estimations, the three-dimensional model and flux model adjoints could also be used to analyse the origins of observed mole-fraction anomalies in terms of specific flux model parameters and initial conditions. This linking of effects to causes enables observation-based corrections to the industry and natural emission models.

Improvements to the driving circulations for CTMs are also needed. The widely used meteorological circulation re-analyses (NCEP, ECMWF, etc.) show significant differences, particularly in regions with very sparse meteorological observations to correct the underlying weather forecasting models.

The modelling of convection and other sub-grid scale phenomena in both chemical transport and weather forecasting models is another area needing significant improvement.

Besides inclusion of all available surface and aircraft measurements of trace-gas mole fractions, future inversions should also include column abundances obtained from satellite and ground-based remote sensing. The above control system approach also enables use of direct measurements of industrial and ecosystem fluxes in the estimation algorithms. Besides accurate calibration comparisons among laboratories, a key issue in combining multiple types of measurements is an accurate estimation of the uncertainties in each type as they will be the basis for the weighting contained in the inverses of the various measurement uncertainty matrices involved in the inversions.

Finally, for GHGs that have natural, anthropogenic, industrial and biogenic emissions, such as CO_2, CH_4 and N_2O, measurements of atmospheric abundances alone are inadequate to differentiate precisely among these different sources. High-frequency *in situ* measurements of not just the total mole fractions of these gases, but also their isotopic compositions are a new frontier in global monitoring and hold the promise of revolutionizing understanding of the natural cycles of these gases and verifying claims of emission reductions. At present, stable isotopic measurements for CO_2 and CH_4 are carried out routinely only by collecting air samples weekly to monthly at network stations for analysis in a central laboratory by conventional gas-source magnetic-sector isotope ratio mass spectrometry, but this sampling frequency is far too limited to be used to accurately constrain estimates of sources and sinks by process and by region. Also, deployment of these instruments at remote stations is inhibited by their high costs, maintenance needs and power requirements, which hinder reliable automation. Measurements of N_2O isotopic composition in the troposphere are even scarcer. Bulk nitrogen-15 (^{15}N) data are available (e.g. [58]), and some intra-molecular ^{15}N measurements have also been made (e.g. [59]).

However, high-frequency *in situ* isotope measurements are now becoming feasible using optical (laser) detection. Recent improvements in mid-infrared quantum cascade lasers (QCL) enable continuous wave (CW) operation near room temperature (RT) with higher power, narrower line widths and higher spectral mode purity than previously possible. The application of CWRT-QCLs has greatly extended detection limits for atmospheric trace-gas measurements without cryogenic cooling of the laser. CWRT-QCLs have been applied to detection of the isotopes of CO_2, CH_4 and N_2O (e.g. [60,61]). In addition to the QCL work, there has been recent progress with isotopic monitoring using other laser sources (e.g. [62,63]). For CH_4 and N_2O, automated cryogenic pre-concentration will probably be necessary to measure their isotopic compositions with the precisions needed to differentiate their various surface fluxes (biogenic, anthropogenic) and photochemical sinks.

The prospects for remote sensing from satellite, aircraft and surface platforms of some of the above isotopomers and isotopologues are less clear, but should also be pursued. These isotopically resolved trace-gas measurements of ambient air would need to be accompanied by accurate field and laboratory measurements of the isotopic signatures of relevant industrial, biological and chemical processes.

Finally, measurements of radiocarbon (^{14}C) are particularly valuable in distinguishing fossil sources of CO_2 and CH_4, but unfortunately the techniques described above do not yet hold promise for measuring ^{14}C in these gases *in situ* with the required high frequency, sensitivity and precision. For the foreseeable future, the highest temporal resolution ^{14}C measurements will probably continue to be made by accelerator mass spectrometry (e.g. [64]), which does not lend itself to *in situ* operation.

5. Conclusions

The examples cited here show that the discrepancies between reported bottom-up GHG emissions and measured top-down accumulations of these emissions in the atmosphere can be substantial. There are many possible explanations for these large discrepancies. Statistical uncertainties in emission factors used in bottom-up protocols are always possible, but such errors ought to be mostly random, and thus do not explain the tendency for the actual emissions to exceed the reported ones, more often than not. When emissions from industrial processes are measured at their sources to establish emission factors, the equipment may be adjusted to minimize emissions, so that the measured values may be lower than they are under typical day-to-day operating conditions, and this would lead to under-reporting. Furthermore, the possible existence of unaccounted or unidentified sources, such as fugitive emissions during industrial production or transportation, would also lead to under-reporting. In addition, the negative impact of GHG emissions on climate, and the financial value of emissions reductions in carbon-equivalent trading markets, both create incentives to under-report actual emissions, whether consciously or subconsciously.

Because effective emissions control legislation ultimately must depend upon enforcement by reliable bottom-up methods, it is essential that these discrepancies be resolved. But since the legislation is national or regional in scale, not global, top-down emission estimates must be determined at these same scales. In addition to recording background GHG trends driven by global and hemispheric emissions, high-frequency atmospheric measurements at well-chosen ground-based station locations also record GHGs that have been elevated above their background values because of regional emissions. By analysing these and other atmospheric measurements with three-dimensional atmospheric transport and mixing models using inverse numerical methods, it is possible to map and quantify regional emissions over time. To reconcile discrepancies between top-down assessments and those obtained by bottom-up protocols, we propose that optimal estimation and control-theory methods be used to identify and correct the most likely causes of the observed discrepancies.

Even with the relatively sparse existing network of ground-based measurement stations, using current modelling techniques, it is possible to rival the accuracies of bottom-up emissions estimates for some GHGs in some regions. Awareness by policy-makers of the large discrepancies which have been found between reported bottom-up emissions and emissions determined from atmospheric measurements has, so far, been limited, but there is an example for European CH_4 emissions in which German CH_4 emissions for 2001 reported to the UNFCCC have been revised upward substantially, and thus were brought into far better agreement with the modelled atmospheric observations [65].

Meeting the goals of effective top-down GHG emissions verification and refining bottom-up protocols to bring about convergence is a research problem that will require substantial increases in the density and scope of atmospheric measurements, as well as improvements in inverse modelling capabilities, but many of the basic components exist already and need only to be increased in scale. Such an initiative would be large when compared with most current atmospheric research programmes, but could easily be supported by an annual investment of less than 1 per cent of the $144 billion US$ currently invested in global carbon-equivalent trading markets [66], with the added benefit of reducing the volatility of these markets and thereby increasing investment in emissions reductions.

We thank the convenors of the Discussion Meeting 'Greenhouse gases in the Earth system: setting the Agenda to 2030' for the opportunity to present our views on this timely issue. We also thank our colleagues in the AGAGE community for their many contributions to the work discussed here, and NASA's Upper Atmosphere Research Program for its continuing support of AGAGE.

References

1 Forster, P. *et al.* 2007 Changes in atmospheric constituents and in radiative forcing. In *Climate change 2007: the physical science basis. Contribution of Working Group I to the Fourth Assessment Report of the Intergovernmental Panel on Climate Change* (eds S. Solomon, D. Qin, M. Manning, Z. Chen, M. Marquis, K. B. Averyt, M. Tignor & H. L. Miller). Cambridge, UK: Cambridge University Press.

2 IPCC. 2006 IPCC Guidelines for National Greenhouse Gas Inventories. Prepared by the National Greenhouse Gas Inventories Programme. In *2006 Institute for Global Environmental Strategies* (*IGES*) (eds H. S. Eggleston, L. Buendia, K. Miwa, T. Ngara & K. Tanabe), Japan. See http://www.ipcc-nggip.iges.or.jp/public/2006gl/index.html.

3 UNFCCC. 2010 National inventory submissions. See http://unfccc.int/national_reports/annex_i_ghg_inventories/national_inventories_submissions/items/5270.php.

4 Enting, I. G. 2002 *Inverse problems in atmospheric constituent transport*. Cambridge, UK: Cambridge University Press.

5 Kasibhatla, P., Heimann, M., Rayner, P., Mahowald, N., Prinn, R. G. & Hartley, D. E. (eds) 2000 *Inverse methods in global biogeochemical cycles*. Geophysical Monograph Series, vol. 114. Washington, DC: American Geophysics Union.

6 Prinn, R. G. 2000 Measurement equation for trace chemicals in fluids and solution of its inverse. In *Inverse methods in global biogeochemical cycles* (eds P. Kasibhatla *et al.*), pp. 3–18. Geophysical Monograph Series, vol. 114. Washington, DC: American Geophysics Union.

7 Chen, Y.-H. & Prinn, R. G. 2005 Atmospheric modeling of high- and low-frequency methane observations: importance of interannually varying transport. *J. Geophys. Res.* **110**, D10303. (doi:10.1029/2004JD005542)

8 Chen, Y.-H. & Prinn, R. G. 2006 Estimation of atmospheric methane emissions between 1996–2001 using a 3D global chemical transport model. *J. Geophys. Res.* **111**, D10307. (doi:10.1029/2005JD006058)

9 Prinn, R. G. *et al.* 2005 Evidence for variability of atmospheric hydroxyl radicals over the past quarter century. *Geophys. Res. Lett.* **32**, L07809. (doi:10.1029/2004GL022228)

10 Mahowald, N. M., Prinn, R. G. & Rasch, P. J. 1997 Deducing CCl_3F emissions using an inverse method and chemical transport models with assimilated winds. *J. Geophys. Res.* **102**, 28 153–28 168. (doi:10.1029/97JD02086)

11 Hartley, D. E. & Prinn, R. G. 1993 On the feasibility of determining surface emissions of trace gases using an inverse method in a three-dimensional chemical transport model. *J. Geophys. Res.* **98**, 5183–5198. (doi:10.1029/92JD02594)

12 Mulquiney, J. E., Taylor, J. A., Jakeman, A. J., Norton, J. P. & Prinn, R. G. 1998 A new inverse method for trace-gas flux estimation. II. Application to tropospheric $CFCl_3$ fluxes. *J. Geophys. Res.* **103**, 1429–1442. (doi:10.1029/97JD01811)

13 Lawrence, M. G., Crutzen, P. J., Rasch, P. J., Eaton, B. E. & Mahowald, N. M. 1999 A model for studies of tropospheric photochemistry: description, global distributions, and evaluation. *J. Geophys. Res.* **104**, 26 245–26 277. (doi:10.1029/1999JD900425)
14 Rasch, P. J., Mahowald, N. M. & Eaton, B. E. 1997 Representations of transport, convection, and the hydrologic cycle in chemical transport models: implications for the modeling of short-lived and soluble species. *J. Geophys. Res.* **102**, 28 127–28 138. (doi:10.1029/97JD02087)
15 Dargaville, R., McGuire, A. D. & Rayner, P. 2002 Estimates of large-scale fluxes in high latitudes from terrestrial biosphere models and an inversion of atmospheric CO_2 measurements. *Clim. Change* **55**, 273–285. (doi:10.1023/A:1020295321582)
16 Gurney, K. R. *et al.* 2002 Towards robust regional estimates of CO_2 sources and sinks using atmospheric transport models. *Nature* **415**, 626–630. (doi:10.1038/415626a)
17 Gurney, K. R. *et al.* 2003 Transcom 3 CO_2 inversion intercomparison. I. Annual mean control results and sensitivity to transport and prior flux information. *Tellus B* **55**, 555–579. (doi:10.1034/j.1600-0889.2003.00049.x)
18 Law, R. M., Chen, Y.-H., Gurney, K. R. & TransCom 3 modellers. 2003 TransCom3 CO_2 inversion intercomparisons. Part 2. Sensitivity of annual mean results to data choices. *Tellus B* **55**, 580–595. (doi:10.1034/j.1600-0889.2003.00053.x)
19 Huang, J. *et al.* 2008 Estimation of regional emissions of nitrous oxide from 1997 to 2005 using multinetwork measurements, a chemical transport model, and an inverse method. *J. Geophys. Res.* **113**, D17313. (doi:10.1029/2007JD009381)
20 Xiao, X. *et al.* 2010 Atmospheric three-dimensional inverse modeling of regional industrial emissions and global oceanic uptake of carbon tetrachloride. *Atmos. Chem. Phys.* **10**, 10 421–10 434. (doi:10.5194/acp-10-10421-2010)
21 Draxler, R. R. & Hess, G. D. 1997 Description of the HYSPLIT_4 modeling system. NOAA Technical Memorandum ERL ARL-224, NOAA Air Resources Laboratory, Silver Spring, MD.
22 Draxler, R. R. & Hess, G. D. 1998 An overview of the HYSPLIT_4 modelling system for trajectories, dispersion and deposition. *Australian Met. Mag.* **47**, 295–308.
23 Kleiman, G. & Prinn, R. G. 2000 Measurement and deduction of emissions of trichloroethene, tetrachloroethene and trichloromethane (chloroform) in the northeastern United States and southeastern Canada. *J. Geophys. Res.* **105**, 28 875–28 893. (doi:10.1029/2000JD900513)
24 Biraud, S., Ciais, P., Ramonet, M., Simmonds, P., Kazan, V., Monfray, P., O'Doherty, S., Spain, T. G. & Jennings, S. G. 2000 European greenhouse gas emissions estimated from continuous atmospheric measurements and radon 222 at Mace, Head Ireland. *J. Geophys. Res.* **105**, 1351–1366. (doi:10.1029/1999JD900821)
25 Derwent, R., Simmonds, P. G., O'Doherty, S., Ciais, P. & Ryall, D. 1998 European source strengths and northern hemisphere baseline concentrations of radiatively active trace gases at Mace Head, Ireland. *Atmos. Environ.* **32**, 3703–3715. (doi:10.1016/S1352-2310(98)00093-4)
26 Derwent, R. G., Simmonds, P. G., O'Doherty, S. & Ryall, D. B. 1998 The impact of the Montreal Protocol on halocarbon concentrations in Northern hemisphere baseline and European air masses at Mace Head, Ireland from 1987–1996. *Atmos. Environ.* **32**, 3689–3702. (doi:10.1016/S1352-2310(98)00092-2)
27 Manning, A. J., Ryall, D. B., Derwent, R. G., Simmonds, P. G. & O'Doherty, S. 2003 Estimating European emissions of ozone-depleting and greenhouse gases using observations and a modeling back-attribution technique. *J. Geophys. Res.* **108**, 4405. (doi:10.1029/2002JD002312)
28 Ryall, D. B., Derwent, R. G., Manning, A. J., Simmonds, P. G. & O'Doherty, S. 2001 Estimating source regions of European emissions of trace gases from observations at Mace Head. *Atmos. Environ.* **35**, 2507–2523. (doi:10.1016/S1352-2310(00)00433-7)
29 Ryall, D. B., Maryon, R. H., Derwent, R. G. & Simmonds, P. G. 1998 Modelling long-range transport of CFCs to Mace Head Ireland. *Q. J. R. Meteor. Soc.* **124**, 417–446. (doi:10.1002/qj.49712454604)
30 Cox, M. L., Sturrock, G. A., Fraser, P. J., Siems, S. T., Krummel, P. B. & O'Doherty, S. 2003 Regional sources of methyl chloride, chloroform and dichloromethane identified from AGAGE observations at Cape Grim, Tasmania, 1998–2000. *J. Atmos. Chem.* **45**, 79–99. (doi:10.1023/A:1024022320985)

31 Wang, Y.-P. & Bentley, S. 2002 Development of a spatially explicit inventory of methane emissions from Australia and its verification using atmospheric concentration data. *Atmos. Environ.* **36**, 4965–4975. (doi:10.1016/S1352-2310(02)00589-7)

32 Stohl, A. *et al.* 2009 An analytical inversion method for determining regional and global emissions of greenhouse gases: sensitivity studies and application to halocarbons. *Atmos. Chem. Phys.* **9**, 1597–1620. (doi:10.5194/acp-9-1597-2009)

33 Cunnold, D. M., Fraser, P. J., Weiss, R. F., Prinn, R. G., Simmonds, P. G., Miller, B. R., Alyea, F. N. & Crawford, A. J. 1994 Global trends and annual releases of CCl_3F and CCl_2F_2 estimated from ALE/GAGE and other measurements from July 1978 to June 1991. *J. Geophys. Res.* **99**, 1107–1126. (doi:10.1029/93JD02715)

34 Hirsch, A. I., Michalak, A. M., Bruhwiler, L. M., Peters, W., Dlugokencky, E. J. & Tans, P. P. 2006 Inverse modeling estimates of the global nitrous oxide surface flux from 1998–2001. *Glob. Biogeochem. Cycles* **20**, GB1008. (doi:10.1029/2004GB002443)

35 Miller, B. R., Weiss, R. F., Salameh, P. K., Tanhua, T., Greally, B. R., Mühle, J. & Simmonds, P. G. 2008 Medusa: a sample preconcentration and GC/MS detector system for *in situ* measurements of atmospheric trace halocarbons, hydrocarbons and sulfur compounds. *Anal. Chem.* **80**, 1536–1545. (doi:10.1021/ac702084k)

36 Prinn, R. G. *et al.* 2000 A history of chemically and radiatively important gases in air deduced from ALE/GAGE/AGAGE. *J. Geophys. Res.* **105**, 17 751–17 792. (doi:10.1029/2000JD900141)

37 Butler, J. H., Battle, M., Bender, M. L., Montzka, S. A., Clarke, A. D., Saltzman, E. S., Sucher, C. M., Severinghaus, J. P. & Elkins, J. W. 1999 A record of atmospheric halocarbons during the twentieth century from polar firn air. *Nature* **399**, 749–755. (doi:10.1038/21586)

38 Rigby, M. *et al.* 2008 Renewed growth of atmospheric methane. *Geophys. Res. Lett.* **35**, L22805. (doi:10.1029/2008GL036037)

39 Dlugokencky, E. J. *et al.* 2009 Observational constraints on recent increases in the atmospheric CH_4 burden. *Geophys. Res. Lett.* **36**, L18803. (doi:10.1029/2009GL039780)

40 Bousquet, P. *et al.* 2006 Contribution of anthropogenic and natural sources to atmospheric methane variability. *Nature* **443**, 439–443. (doi:10.1038/nature05132)

41 Mühle, J. *et al.* 2010 Perfluorocarbons in the global atmosphere: tetrafluoromethane, hexafluoroethane, and octafluoropropane. *Atmos. Chem. Phys.* **10**, 5145–5164. (doi:10.5194/acp-10-5145-2010)

42 Deeds, D. A., Mühle, J. & Weiss, R. F. 2008 Tetrafluoromethane in the deep North Pacific Ocean. *Geophys. Res. Lett.* **35**, L14606. (doi:10.1029/2008GL034355)

43 IAI. 2009 The International Aluminium Institute Report on the aluminium industry's global perfluorocarbon gas emissions reduction programme. Results of the 2008 Anode Effect Survey. International Aluminium Institute, London, UK.

44 EDGAR. 2009 *Emission database for global atmospheric research, release v. 4.0.* European Commission, Joint Research Centre/Netherlands Environmental Assessment Agency. See http://edgar.jrc.ec.europa.eu.

45 Vollmer, M. K. & Weiss, R. F. 2002 Simultaneous determination of sulfur hexafluoride and three chlorofluorocarbons in water and air. *Mar. Chem.* **78**, 137–148. (doi:10.1016/S0304-4203(02)00015-4)

46 Levin, I. *et al.* 2010 The global SF_6 source inferred from long-term high precision atmospheric measurements and its comparison with emission inventories. *Atmos. Chem. Phys.* **10**, 2655–2662. (doi:10.5194/acp-10-2655-2010)

47 Maiss, M. & Levin, I. 1994 Global increase of SF_6 observed in the atmosphere. *Geophys. Res. Lett.* **21**, 569–572. (doi:10.1029/94GL00179)

48 Rigby, M. *et al.* 2010 History of atmospheric SF_6 from 1973 to 2008. *Atmos. Chem. Phys.* **10**, 10 305–10 320. (doi:10.5194/acp-10-10305-2010)

49 Geller, L. S., Elkins, J. W., Lobert, J. M., Clarke, A. D., Hurst, D. F., Butler, J. H. & Myers, R. C. 1997 Tropospheric SF_6: observed latitudinal distribution and trends, derived emissions and interhemispheric exchange time. *Geophys. Res. Lett.* **24**, 675–678. (doi:10.1029/97GL00523)

50 Peters, W. *et al.* 2004 Toward regional-scale modeling using the two-way nested global model TM5: characterization of transport using SF_6. *J. Geophys. Res.* **109**, D19314. (doi:10.1029/2004JD005020)

51 Maiss, M. & Brenninkmeijer, C. M. 1998 Atmospheric SF_6: trends, sources, and prospects. *Environ. Sci. Technol.* **32**, 3077–3086. (doi:10.1021/es9802807)

52 Prather, M. J. & Hsu, J. 2008 NF_3, the greenhouse gas missing from Kyoto. *Geophys. Res. Lett.* **35**, L12810. (doi:10.1029/2008GL034542)

53 Weiss, R. F., Mühle, J., Salameh, P. K. & Harth, C. M. 2008 Nitrogen trifluoride in the global atmosphere. *Geophys. Res. Lett.* **35**, L20821. (doi:10.1029/2008GL035913)

54 Lee, J.-Y., Lee, J. B., Moon, D. M., Souk, J. H., Lee, S. Y. & Kim, J. S. 2007 Evaluation method on destruction and removal efficiency of perfluorocarbons from semiconductor and display manufacturing. *Bull. Korean Chem. Soc.* **28**, 1383–1388. (doi:10.5012/bkcs.2007.28.8.1383)

55 Mühle, J. *et al.* 2009 Sulfuryl fluoride in the global atmosphere. *J. Geophys. Res.* **114**, D05306. (doi:10.1029/2008JD011162)

56 Papadimitriou, V. C., Portmann, R. W., Fahey, D. W., Mühle, J., Weiss, R. F. & Burkholder, J. B. 2008 Experimental and theoretical study of the atmospheric chemistry and global warming potential of SO_2F_2. *J. Phys. Chem. A.* **112**, 12657–12666. (doi:10.1021/jp806368u)

57 Wunsch, C. 1996 *The ocean circulation inverse problem.* New York, NY: Cambridge University Press.

58 Rahn, T. & Wahlen, M. 1997 Stable isotope enrichment in stratospheric nitrous oxide. *Science* **278**, 1776–1778. (doi:10.1126/science.278.5344.1776)

59 Kaiser, J., Röckmann, T. & Brenninkmeijer, C. A. M. 2003 Complete and accurate mass spectrometric isotope analysis of tropospheric nitrous oxide. *J. Geophys. Res.* **108**, 4476. (doi:10.1029/2003JD003613)

60 Nelson, D., McManus, J., Herndon, S., Zahniser, M., Tuzson, B. & Emmenegger, L. 2008 New method for isotopic ratio measurements of atmospheric carbon dioxide using a 4.3 μm pulsed quantum cascade laser. *Appl. Phys., B Lasers Opt.* **90**, 301–309. (doi:10.1007/s00340-007-2894-1)

61 Nelson, D. D., McManus, J. B., Urbanski, S., Herndon, S. & Zahniser, M. S. 2004 High precision measurements of atmospheric nitrous oxide and methane using thermoelectrically cooled mid-infrared quantum cascade lasers and detectors. *Spectrochim. Acta A* **60**, 3325–3335. (doi:10.1016/j.saa.2004.01.033)

62 Castrillo, A., Casa, G., Kerstel, E. & Gianfrani, L. 2005 Diode laser absorption spectrometry for $^{13}CO_2/^{12}CO_2$ isotope ratio analysis: investigation on precision and accuracy levels. *Appl. Phys., B Lasers Opt.* **81**, 863–869. (doi:10.1007/s00340-005-1949-4)

63 Waechter, H. & Sigrist, M. 2007 Mid-infrared laser spectroscopic determination of isotope ratios of N_2O at trace levels using wavelength modulation and balanced path length detection. *Appl. Phys., B Lasers Opt.* **87**, 539–546. (doi:10.1007/s00340-007-2576-z)

64 Graven, H. D., Guilderson, T. P. & Keeling, R. F. 2007 Methods for high-precision ^{14}C AMS measurement on atmospheric CO_2 at LLNL. *Radiocarbon* **49**, 349–356.

65 Bergamaschi, P., Krol, M., Dentener, F., Vermeulen, A., Meinhardt, F., Graul, R., Ramonet, M., Peters, W. & Dlugokencky, E. J. 2005 Inverse modelling of national and European CH_4 emissions using the atmospheric zoom model TM5. *Atmos. Chem. Phys.* **5**, 2431–2460. (doi:10.5194/acp-5-2431-2005)

66 Kossoy, A. & Ambrosi, P. 2010 *State and Trends of the Carbon Market 2010.* Washington, DC: The World Bank.